FERMILAB-CONF-76-150-E

Further Results on Neutrino Interactions in Hydrogen using the Fermilab fifteen foot Bubble Chamber

C.T. Coffin, R.N. Diamond, H.T. French. W.Louis, B.P. Roe, A.A. Seidl, J. Vander Velde, Univ. of Michigan; J.P. Berge, D.V. Bogert, D.C. Cundy*, F.A. DiBianca, V. Efremenko‡, H. Emans#, P. Ermolov‡, R. Hanft, C. Kochowski‡, M.A. Kubantsev†, F.A. Nezrick, Y. Rjabov‡, W.G. Scott, W. Smart, Fermilab; R.J. Cence, F.A. Harris, S.I. Parker, M.W. Peters, V. Z. Peterson, V.J. Stenger, Univ. of Hawaii; A. Barbaro-Galtieri, G.R. Lynch, J.P. Marriner, F.T. Solomitz, M.L. Stevenson, Lawrence Berkeley Laboratory.

Presented to the XVIII International Conference on
High Energy Physics
Tbilisi -- July 15-21, 1976

submitted by B. Roe

*Permanent address: CERN, Geneva, Switzerland

#Permanent address: Univ. of Bonn, Bonn, W. Germany

‡Permanent address: IHEP, Serpukhov, USSR

‡Permanent address: SEN, Saclay, France

†Permanent address: ITEP, Moscow, USSR

In this paper we will discuss five topics: limits on production of known meson resonances, properties of neutral current events, some inclusive properties of charged current events, $\Delta(1232)$ production, and searches for exotic interactions.

We have obtained a sample of charged and neutral current neutrino interactions with free protons using the Fermilab fifteen foot bubble chamber filled with hydrogen. The neutrino beam was a broad band beam produced by 300 GeV/c protons and focussed by one horn. Approximately 75000 pictures were used in the present analysis.

An external muon identifier (EMI) consisting of a single $25m^2$ plane of proportional wire chambers behind 3 to 4 absorption lengths of material was operated in conjunction with the bubble chamber. It is essential to make use of the EMI information in order to obtain a reasonably pure sample of neutral current events (section III). For the other sections (unless indicated otherwise) the muon selection and event reconstruction was by the BCM method.[1] In this method the muon is chosen to be the negative track with highest momentum transverse to the neutrino beam direction. An attempt is then made to reconstruct the event to estimate the neutrino energy. To do this the assumption is made that the direction of total hadronic momentum is essentially in the direction of the visible hadronic momentum. More precisely it is assumed that the direction of total hadronic momentum is the projection of the visible hadronic momentum onto the plane formed by the muon and neutrino momentum vectors. With this assumption the total energy can be estimated by transverse momentum balance.

#454

Some events fail to reconstruct by this method and are rejected as charged current candidates. This happens if the muon and hadron momentum vectors are on the same side of the neutrino momentum direction, i.e., if the angle between the component of the muon momentum perpendicular to the neutrino directionand the component of the total visible hadron momentum perpendicular to the neutrino direction is greater than 90°.

An examination of the reliability of this method and the purity of the sample thus obtained is given in reference 1. We find there that use of this method results in an 86% pure charged current sample. The energy resolution of the neutrino energy estimate is such that 50% of the events have errors of less than 8%.

I. Search for Known Meson Resonances Produced in Neutrino Proton Interactions.

For this search we have used a sample of about 500 charged current neutrino events with visible momentum in the beam direction (ΣP_x) greater than 10 GeV/c. The EMI was used to help identify the muon for the B and $\omega°$ search only. For these events if the EMI indicated the probability of a track being a hadron was less than 10% and the probability of that track being a muon was greater than 4%, the track was taken as a muon. For the other channels and for those events in the B and $\omega°$ channel without EMI identification the muon was chosen to be the negative track with highest momentum transverse to the neutrino direction.

One charged current event corresponds crudely to 4×10^{-40} cm^2 at our mean neutrino energy of 38 GeV if the cross section is proportional to laboratory energy. If the cross section is constant above $E_\nu = 10$ GeV one event corresponds to about $3 \times 10^{-40} cm^2$.

We wish to search for resonances in some neutral current channels also. For the neutral current sample we require the visible momentum in the beam direction to be greater than 5 GeV/c. For the present purposes we accept an event as a neutral current candidate if it fails to reconstruct as a charged current event. About 55% of the neutral current events are expected to fail this reconstruction. For neutral currents the above cross section per event thus should be multiplied by 1.82.

In some of the channels to be discussed below we have restricted the sample to events with an identified proton below 1 GeV/c.

We have estimated our efficiency for identifying a track as a proton by examining how often we identified a track as a proton in events which turned out to have no missing outgoing neutrals, since we could make constrained fits (3C) to these events. Furthermore, we chose to compare only with events having no electron pairs or kinks, having fits to neutrino interactions involving only protons and pions in the final state and having a confidence level of greater than 5% for the fit. For the present events we find that we identify 94 ± 6% of the protons below .5 GeV/c and 48 ± 10% of the protons between .5 and 1 GeV/c. These numbers will be improved shortly due to a more sophisticated track fitting method. We found no examples of a track being chosen as a proton, which after kinematic fitting of the event was found not to be a proton. If the proton momentum distribution goes as $\sim e^{-6t}$ ($t = 2M_pKE_p$) typical of hadronic diffractive processes than about 92% of the proton diffractive events will be below 1 GeV/c and be identified.

Channels with 1 π° correspond to a 0-C fit, i.e., no constraints. Nonetheless, a number of events cannot be reconstructed as 1 π° events. The events which can be reconstructed in this manner contain a large number of 2 π° or 3 π° events which add to the background.

Figures 1 and 2 show the results of searching for meson resonances in several channels. The events in 2a and 2b are the same events with the charged non-proton tracks taken to have π and k masses respectively. We have observed no signal above background in any channel we have searched to date. The number of

events in various mass bins for the appropriate resonance are given in table I. In all cases these are no higher than the general background.

Most of the events in the ρ region have the mass of the π + p in the $\Delta(1232)$ region. Relaxing the proton criteria allows more events. However, no peak starts to appear and the events have considerally more contamination.

There have been several calculations[2,3,4] for the ρ and A_1 cross sections. Although the assumptions are similar the results vary by several orders of magnitude. We have considerably fewer events than predicted by Gaillard, are getting uncomfortably low for Stodolsky and Piketty, but our upper limit is still above the value predicted by Roe.

If we look at the three pion ($\pi^+\pi^+\pi^-$) effective mass for specifically non-diffractive events a possible enchancement above Monte Carlo predictions in the .8 - 1.3 GeV/c^2 mass region is seen. (fig. 3) Here we have selected all five charged prong events of the form $\nu p \rightarrow \mu^- p\ \pi^+\pi^+\pi^-\ x$. A somewhat relaxed proton criterion was used for this plot. The t distribution indicates the non-diffractive nature of the enhancement as does the fact that it appears only in events with missing neutrals (x not 0). Because of possible contamination of the sample of protons and because of the paucity of statistics this effect is not yet on firm footing. The data for this plot are taken from a slightly larger sample of events than the data in figures 1 and 2.

II. Neutral Current Events

For this study we use the 70% of the total data sample in which the EMI was in reliable operation. We have attempted to select out a sample of neutral current candidates to examine their properties. The philosophy followed was to reject an event if it could be a charged current candidate.

We start with 639 neutrino event candidates with total visible momentum in the beam direction greater than 5 GeV/c.

An event is taken to be a neutral current candidate if it satisfies the following criteria:

a) No track is signalled as a non-hadron by the EMI, i.e., we ask that the confidence level for being a hadron $\equiv C_h > .07$.

b) The event satisfies at least one of the following three criteria:

1. The event fails to reconstruct using the BCM[1] reconstruction method.
2. The event reconstructs but in such a manner that the invisible neutrals carry away more than 60% of the neutrino momentum in the neutrino beam direction or more than 10% in the backward direction.
3. All tracks have $C_h > .07$, i.e., all tracks pass through the EMI and a.) is satisfied.

c) The confidence level for each track that passes through the EMI to be a muon $\equiv C_\mu < .2$.

d) No track taken as a muon has more than 2 GeV/c momentum transverse to the direction of the sum of the momentum of all of the other tracks.

318 events are left. The above cuts are designed to remove charged current background from the sample. Therefore, we have lost a considerable number of the neutral current events (30 to 50%). These losses are included in the Monte Carlo curves which will be shown with the data.

The neutron and K_L° background have been evaluated previously[1]. It is clear that the background is low for $\Sigma P_x > 5$ GeV/c. We estimate the neutron background to be about 12% above 5 GeV/c. At present we have only upper limits for the K_L° background. It is possible that the neutron and K_L° contamination is more serious below the 5 GeV/c range and we are investigating this point further.

The distribution of charged prong multiplicity for the neutral current events in our sample is shown in fig. 4. We have almost equal numbers of 3 and 5 prong events with only about 20% of the events having higher multiplicity. The visible energy distribution is shown in fig. 5. This is compared with Monte Carlo events generated assuming the quark-parton model, the experimental charged current results for the x distribution and the momentum of hadrons within the hadron jet, and for different neutral current possibilities[5]. We have not included our data below 6 GeV in the $E_{visible}$ plot because we have not yet proven the neutron and K_L° contamination is low. If further calculations show this region to have a low contamination then as can be seen, we might hope to have some ability to discriminate among some of the various neutral current possibilities.

We have examined the distribution of $P_\perp$, the momentum of an individual hadron transverse to the direction of the visible hadron

system. (Fig. 6). The result is quite consistent with the result for charged currents. Figure 7 shows the distribution of $Z^{\pm}_{vis}$, the fraction of the visible energy carried by positive and negative hadrons in neutral current interactions. The comparison curve is for Z, the fraction of total energy (rather than visible energy) carried by individual hadrons. Again, the data agree with charged current neutrino results and with calculations from electroproduction data[6]. The excess for negatives at high Z is perhaps due to charged current contamination of our neutral current sample.

Finally some hadronic effective mass distributions are shown in fig. 8 and are compared with Monte Carlo results. No obvious resonances appear. The proton criterion used is less stringent than used for most of section I. Here the momentum of the proton candidate was required to be less than 1.5 GeV/c and the residuals for fitting the track as a proton were required to be at least 5% better than the residuals for fitting the track as a pion.

III. Multiparticle and Inclusive Distributions

We have continued to examine inclusive distributions for our charged current sample and compare them with comparable photoproduction, electroproduction, and hadroproduction data. We use here a $\Sigma P_x > 5$ GeV/c cut. $S = W^2 =$ the mass squared of the hadronic system.

In fig. 9 we show the invariant cross section for negative hadrons as a function of Feynman X ($X = \frac{P^*_{\parallel}}{P^*_{\parallel max}}$). Here we have selected events with $Q^2 < 32$ (GeV/c^2).

Figure 10 shows the corresponding data for hadron interactions[7] and photon interactions[8]. It is clear these are in good

agreement with the neutrino data. In fig. 11 we compare our data for the same invariant cross section with electroproduction data[9]. Again the agreement is quite good.

We next examine the ratio of positive to negative hadrons (R) in the current fragmentation region. We consider events with the effective mass squared of the hadron system (s) greater than 4 GeV^2 and consider those particles with rapidity greater than -1.0 in the quark frame. Effectively this corresponds to choosing Feynman x greater than 0 as is seen in fig. 12.

Figure 13 shows this ratio as a function of $\omega = \frac{1}{x}$. For electroproduction R is in the range of 2 to 3. Since we expect the outgoing current fragments to have a similar charge for both neutrinos and electroproduction the results are in good agreement.

We have previously compared our multiplicity data to the multiplicity in M using pp → p + M diffractive production. We compared the data as a function of the mass of the produced hadronic system obtaining good agreement. Good agreement is also obtained if we compare our multiplicity distribution to the total multiplicity in p-p collisions at a given center of mass energy.

To attempt to distinguish between these two possibilities we have examined the second moment, $f_2 = \langle n^2 \rangle - \langle n \rangle^2 - \langle n \rangle$. See fig. 14. The data seem to favor comparison with p-p total multiplicity.

IV. Δ(1232) Production

We have examined our data for all events which fit $\nu p \rightarrow \mu^- p \pi^+$. This is a three constraint fit. We accepted events with a chi-squared less than 11.

The $\pi^+ p$ effective mass is shown in fig. 15. It is clear the reaction is dominated by the production of Δ(1232). From looking at the events at masses above the 1232 resonance a sum rule limit on the coupling to the weak current of other nucleon resonances decaying to $\pi^+ p$ below 2 GeV/c compared to the Δ(1232) of about 22% is obtained.

For further work we accepted all events above $\Sigma P_x = 5$ GeV/c. The energy distribution is such that the cross section is consistent with being flat although the evidence is not compelling, (fig. 16). Figure 16a shows the number of charged current neutrino events of all kinds divided by energy. Figure 16b shows the number of $\mu^- \pi^+ p$ events (with $M_{\pi^+ p} < 1.4$ GeV/c) versus energy. These graphs should have the same shape for a constant Δ(1232) cross section.

The Q^2 distribution for events in the mass region $M_{\pi^+ p} < 1.4$ GeV/c^2 is shown in fig. 17. The lines correspond to the Adler[10] predictions for $M_A = .96$ GeV/c^2 and $F_\nu = 20$ GeV. We have attempted to normalize them to our data absolutely using the measured νp total cross section results[11] and the measured neutron to proton cross section measurements[12]. We normalize to the data within the $15 < E_\nu < 35$ GeV region. The curves shown correspond to plus and minus one standard deviation for the normalization. The errors are calculated assuming quoted experimental errors. We

assume the total cross section is linear with neutrino energy between CERN and Fermilab energies and that the ratio of cross sections from neutrons and protons remains constant.

V. Search for Exotic Events

We have previously reported[13] an upper limit of 3.6% on inclusive Λ° production via a $\Delta S = -\Delta Q$ current (90% confidence level). We have not found any events fitting exclusive $\Delta S = -\Delta Q$ channels with no missing neutrals.

We have searched our events with vees for possible mass peaks. We have observed no exotic signal greater than 7 events above background.

If f_R is the fraction of our neutrino events containing a "charmed" meson resonance M_c or "charmed" baryon resonance B_c then the upper limits for $\Gamma \lesssim 50$ MeV/c^2 are:

$$f_{M_c} * \text{B.R. } (M_c \rightarrow K_s^\circ + \text{charged pions}) \lesssim 2\%$$

$$f_{B_c} * \text{B.R. } (B_c \rightarrow \Lambda + \text{charged pions}) \lesssim 2\%$$

$$f_{B_c} * \text{B.R. } (B_c \rightarrow pK_s^\circ + \text{charged pions}) \lesssim 2\%$$

We did, however, observe a standard resonance in this search, the Σ(1385) (see fig. 18). If we correct for the branching ratio into $\Lambda\pi$ we find that about 4% of all our charged current events have a Σ(1385). If the production cross section is approximately independent of energy this amounts to about $(.6 \pm .3) \times 10^{-38}$ cm. for the inclusive cross section.

We have searched for short lifetime neutral particles by examining whether the primary vertex in our events could in fact

be a double vertex. We found no such events with our sample. We determined that on the average we could distinguish two vertices if they were 3.5 mm apart. This implies a 90% confidence level limit of $\tau < 8 \times 10^{-12}$ seconds (2% production rate)

$< 5 \times 10^{-12}$ seconds (5% production rate)

From about one-half of our candidates we searched for kinking particles with a high missing transverse momentum at the kink vertex which would be inconsistent with Σ, K, π decay, or with low transverse momentum elastic scattering with an invisibly short proton stub. No such "charmed" hadron decays were found. This corresponds to $f_{H_c} *$ B.R. ($H_c \rightarrow$ kink of high P_T) < 1.5% (90% confidence level).

We have searched for even prong vertices corresponding to particle decays. Except for two prong vertices compatible with gamma, K°, Λ°, or $\bar{\Lambda}^\circ$ none were found. Since if present these could have been induced by events in the chamber wall we have a larger flux to which to normalize our data. The limits are shown in table II.

We do have two events worth noting. We have one event with ΣP_x of 19 GeV/c which has a clear $\bar{\Lambda}^\circ$. For hadron collisions of comparable center of mass energy the ratio $\Lambda^\circ/\bar{\Lambda}^\circ$ is about 0.1%[14] yet we have one $\bar{\Lambda}$ event and only 20 Λ events. We also have one event with 3 vees. The ΣP_x for this event is 29 GeV. One vee is a Λ, one is a K°, and one is ambiguous between Λ and K°. One charged track of momentum 830 MeV/c fits the track reconstruction program better with a K^+ than a π^+ as the hypothesis. The event thus appears to be double associated production.

One way to get enhanced ratios of these classes of events would be to have exotic particles produced in the neutrino interaction which then decay preferentially into strange particles.

With only two events these data are simply a curiosity. We are presently analyzing a sample about four times greater than the sample reported on here and soon perhaps will be able to determine whether this effect persists.

Figure Captions

Fig. 1. Effective masses of groups of pions for various charged current neutrino interactions.

Fig. 2. (a), (b) Effective masses of π and k pairs in the three prong neutral current event candidates.

(c) Search for $\nu p \to \mu^- N^*(1232)\ \rho^\circ + x$. Scatter gram of mass of $\pi_1^+ p$ versus $\pi_2^+\pi^-$ for five prong events.

Fig. 3. (a) Mass of $\pi^+\pi^+\pi^-$ for five prong events $\nu p \to \mu^-\pi^+\pi^+\pi^- p + x$ where x is not zero. The solid histogram is for events fitting $\nu p \to \mu^-\pi^+\pi^+\pi^- p$. The curve is from a Monte Carlo calculation of this distribution using assumptions outlined in Section III.

(b) t distribution for events with $.8 \le M(\pi^+\pi^+\pi^-) < 1.3\ \mathrm{GeV}/c^2$.

Fig. 4. Visible prong distribution for neutral current candidates.

Fig. 5. Visible energy distribution for neutral current event candidates. The curves are from Monte Carlo calculations using various neutral current forms as indicated in the text.

Fig. 6. Distribution of momentum squared of an individual hadron transverse to the overall visible hadron momentum vector.

Fig. 7. Distribution of Z_{vis} the ratio of energy of an individual hadron to the total visible hadronic energy. The solid histogram refers to positive tracks, the dashed histogram to negative tracks, and the straight line shows the Z distribution of positives in electroproduction.

Fig. 8. (a) Distribution of effective masses of x^+ in $\nu p \to \nu x^+$

(b) Distribution of effective masses of x° in $\nu p \to \nu p x^\circ$

(c) Distribution of effective masses of x^- in $\nu p \to \nu \pi^+ p x^-$

Fig. 9. The normalized invariant inclusive cross section for negative hadrons as a function of Feynman X ($X = P^*_{\parallel} / P^*_{\parallel max}$). The x's correspond to the effective mass squared of the hadrons in the 4-16 (GeV/c^2) range and the circles correspond to effective mass squared in the 16-100 $(\mathrm{GeV}/c^2)^2$ range.

Fig. 10. Normalized invariant inclusive cross sections for the production of negative hadrons in photoproduction and hadroproduction as a function of Feynman X. The closed circles correspond to hadroproduction in the effective mass squared range 1-20 $(\mathrm{GeV}/c^2)^2$ and the open circles to hadroproduction in the effective mass squared range 20-50 $(\mathrm{GeV}/c^2)^2$. The line corresponds to photoproduction data at $S = M^2 = 18.3\ (\mathrm{GeV}/c^2)^2$.

Fig. 11. Normalized invariant inclusive cross sections for the production of negative hadrons in neutrino and electroproduction. (Note the cross section here has an extra factor of $\frac{1}{\pi}$ compared to fig. 8 and 9.) The x's and open circles correspond to neutrino production with effective mass squared regions 4-16 $(\mathrm{GeV}/c^2)^2$ and 16-100 $(\mathrm{GeV}/c^2)^2$ regions respectively. The closed circles correspond to electroproduction data with effective mass between 3.5 and 5.5 GeV/c^2 and Q^2 between 2 and 3 $(\mathrm{GeV}/c)^2$.

Fig. 12. Distribution of hadrons as a function of Feynman X. The open histrogram shows the distribution for all hadrons and the shaded histogram for those hadrons with rapidity in the quark frame greater than -1.

Fig. 13. Distribution of the ratio of positive to negative hadrons as a function of $\omega = 1/x$. Events are required to have effective visible hadronic mass squared greater than 4 $(GeV/c^2)^2$ and individual particles are required to have rapidity greater than -1 in the quark frame.

Fig. 14. Distribution of $f_2 = \langle n^2 \rangle - \langle n \rangle^2 - \langle n \rangle$ as a function of hadronic visible effective mass squared where m is the multiplicity of charged hadrons. The data points correspond to neutrino events, the solid line to X^+ in $pp \to pX^+$ in 100 GeV/c proton collisions, and the dashed line to p-p total multiplicity at center of mass energy squared=$s=M^2$.

Fig. 15. Distribution of π^+p effective masses for the reaction $\nu p \to \mu^-\pi^+p$.

Fig. 16. (a) Number of charged current events divided by energy as a function of neutrino energy.
(b) Number of $\nu p \to \mu^\circ\pi^+p$ events with $M_{\pi^+p} < 1.4$ GeV/c^2 as a function of neutrino energy.

Fig. 17. Number of events $\nu p \to \mu^-\pi^+p$ with $M_{\pi^+p} < 1.4$ GeV/c^2 as a function of Q^2. The lines represent the plus or minus one standard deviation normalization limits for the Adler prediction as described in the text.

Fig. 18. Distribution of $\Lambda\pi^+$ effective mass for events of the form $\nu p \to \mu^-\Lambda\pi^+X$.

References

1. J. W. Chapman et al. Phys. Rev. in press
2. B. P. Roe, Phys. Rev. Lett. 21 1666 (1968), Erratum 22 92 (1969)
3. C. A. Piketty and L. Stodolsky, Nuc. Phys. B15 571 (1970)
4. M. K. Gaillard, S. A. Jackson and D. V. Nanopoulos, CERN preprint TH. 2049 - CERN, July 1975
5. S. Pakvasa, private communication
6. L. M. Sehgal, Nuc. Phys. B90 471 (1975)
7. J. P. deBrion et al, Phys. Lett. B52 477 (1974)
8. K. Moffeit et al. Phys. Rev. D5 1605 (1972)
9. J. T. Daken et al. Phys. Rev. D10 1401 (1974)
10. P. Schreiner and F. Von Hippel, Nuc. Phys. B58 333 (1973)
11. B. C. Barish et al. Phys. Rev. Lett. 35 1316 (1975)
12. Quoted by D. Perkins, SLAC Conference Proceedings, 580 (1975)
13. J. P. Berge et al. Phys. Rev. Lett. 36 639 (1976)
14. K. Kleinknecht, private communication

Tables

Table I. Limits for Various Diffractive Channels

Table II. Limits on Exotic Neutral Particle Decays

Table I

Reaction	Identified proton required	Bin (GeV/c^2)	Number of entries	Comments
$\nu p \to \mu^- p\ \rho^+ \hookrightarrow \pi^+\pi^\circ$	yes	.6 - .7 .7 - .8 .8 - .9	2 2 3	
$\nu p \to \mu^- p\ A_1^+ \hookrightarrow \pi^+\pi^+\pi^-$	no	1.0 - 1.2	3	For this limit we use the 15 kinematically fitted (3C) $\nu p \to \mu^- p \pi^+ \pi$ events in our sample.
$\nu p \to \mu^- p \pi^+ \omega^\circ \hookrightarrow \pi^+\pi^-\pi^\circ$	no	.7 - .9	39	We have 6 combination event here. Certain < 20 of these events could be ω°.
$\nu p \to \mu^- p B \hookrightarrow \pi^+\omega^\circ$	no	ω° .7 - .9 B 1.2 - 1.3	5	
$\nu p \to \nu p\ \rho^\circ \hookrightarrow \pi^+\pi^-$	yes	.6 - .8 .8 - 1.0	1 3	
$\nu p \to \nu p\ \phi \hookrightarrow K^+K^-$	yes	.8 - 1 1 - 1.2	0 2	
$\nu p \to \nu \Delta(1232)\ \rho^\circ \hookrightarrow \pi^+\pi^-$, $\Delta \hookrightarrow \pi^+ p$	yes *	ρ° .7 - .9 $\Delta(1232)$ 1.2-1.3	2	2 combination/event

Table II

$\bar{\ell}$ DECAY (m.)	IN-CHAMBER DECAY PROBABILITY	$\frac{\sigma(\nu Nuc \to \text{new particle}) \times BR(\geq 4 \text{ prongs})}{\sigma_{TOT}(\nu Nuc)}$	$\frac{\sigma(\nu p \to \text{new particle}) \times BR(2 \text{ prongs})}{\sigma_{TOT}(\nu p)}$	IN-CHAMBER DECAY PROBABILITY	$\bar{\ell}$ DECAY (m.)
0.01	0.005	$< 2 \times 10^{-1}$	$< 6 \times 10^{-3}$	1.0	0.01
0.10	0.050	$< 2 \times 10^{-2}$	$< 7 \times 10^{-3}$	0.95	0.10
1.0	0.27	$< 4 \times 10^{-3}$	$< 1.2 \times 10^{-2}$	0.56	1.0
10.0	0.09	$< 1 \times 10^{-2}$	$< 7.4 \times 10^{-2}$	0.09	10.0

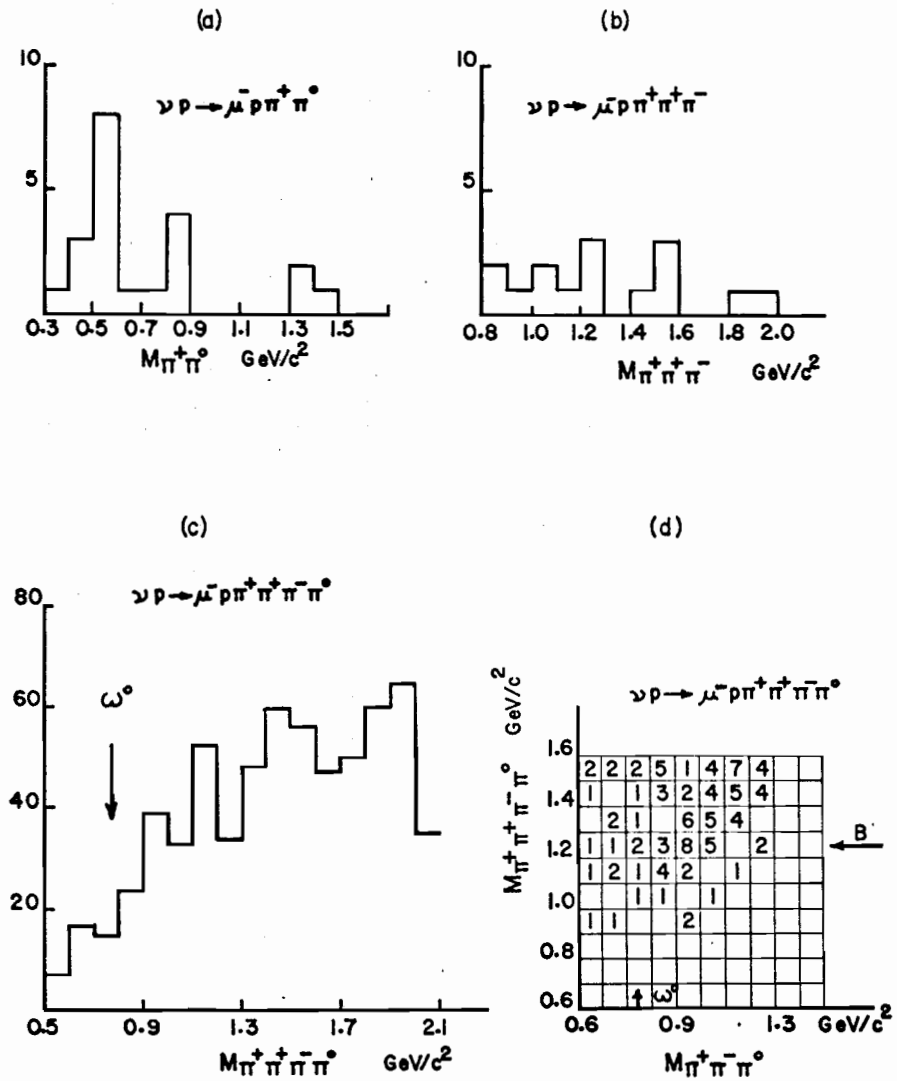
(a)
$\nu p \to \mu^- p \pi^+ \pi^0$
$M_{\pi^+\pi^0}$ GeV/c^2
(b)
$\nu p \to \mu^- p \pi^+ \pi^+ \pi^-$
$M_{\pi^+\pi^+\pi^-}$ GeV/c^2
(c)
$\nu p \to \mu^- p \pi^+ \pi^+ \pi^- \pi^0$
ω^0
$M_{\pi^+\pi^+\pi^-\pi^0}$ GeV/c^2
(d)
$\nu p \to \mu^- p \pi^+ \pi^+ \pi^- \pi^0$
$M_{\pi^+\pi^-\pi^0}$ GeV/c^2
$M_{\pi^+\pi^-\pi^0}$ GeV/c^2
B
ω^0

fig. 1

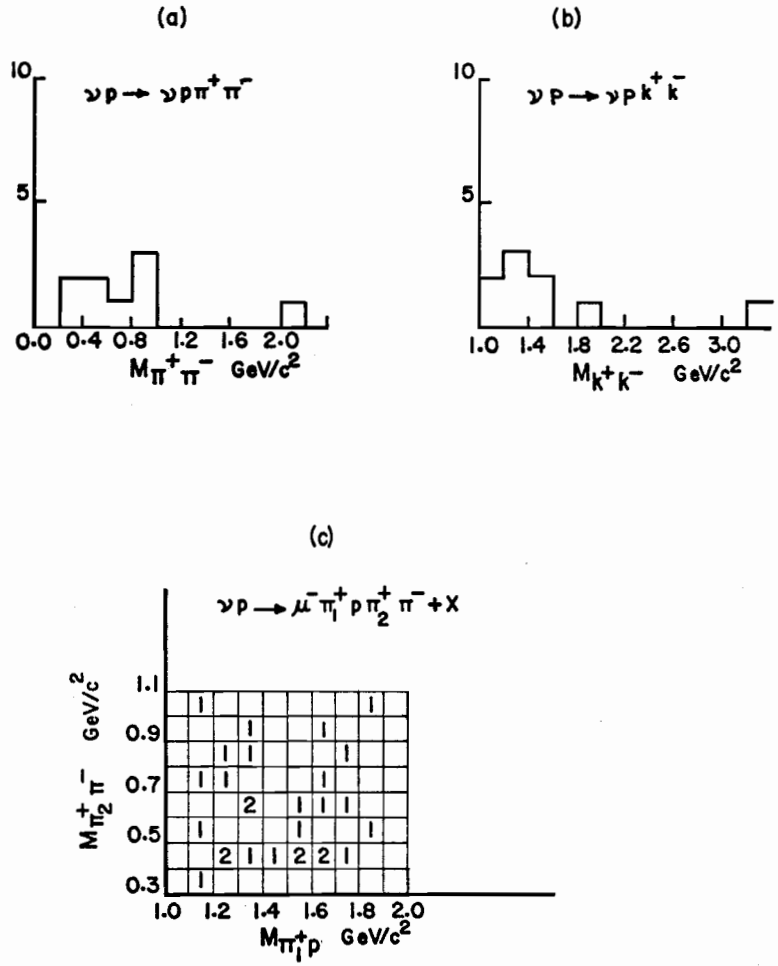
(a)
$\nu p \to \nu p \pi^+ \pi^-$
$M_{\pi^+\pi^-}$ GeV/c^2
(b)
$\nu p \to \nu p k^+ k^-$
$M_{k^+k^-}$ GeV/c^2
(c)
$\nu p \to \mu^- \pi_1^+ p \pi_2^+ \pi^- + X$
$M_{\pi_2^+\pi^-}$ GeV/c^2
$M_{\pi_1^+ p}$ GeV/c^2

fig. 2

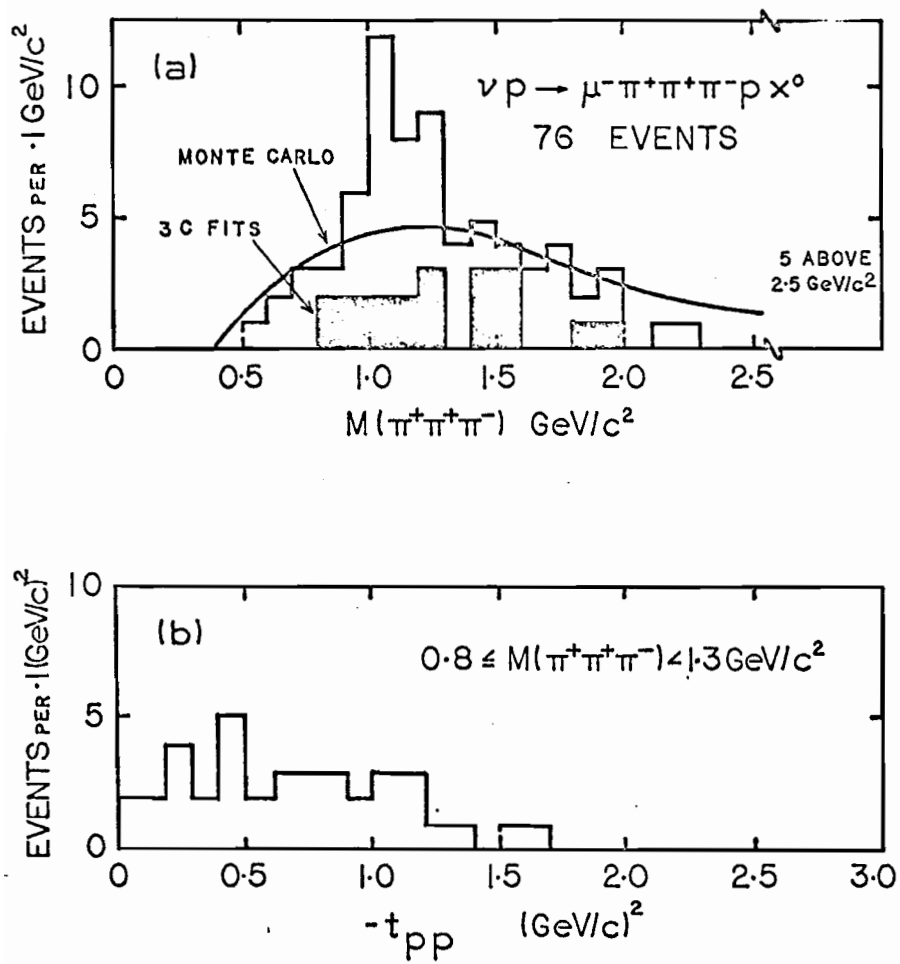
(a)
$\nu p \rightarrow \mu^- \pi^+ \pi^+ \pi^- p x^0$
76 EVENTS
MONTE CARLO
3 C FITS
5 ABOVE
2·5 GeV/c²
EVENTS PER ·1 GeV/c²
M(π⁺π⁺π⁻) GeV/c²
(b)
0·8 ≤ M(π⁺π⁺π⁻) < 1·3 GeV/c²
EVENTS PER ·1 (GeV/c)²
-t_pp (GeV/c)²

fig. 3

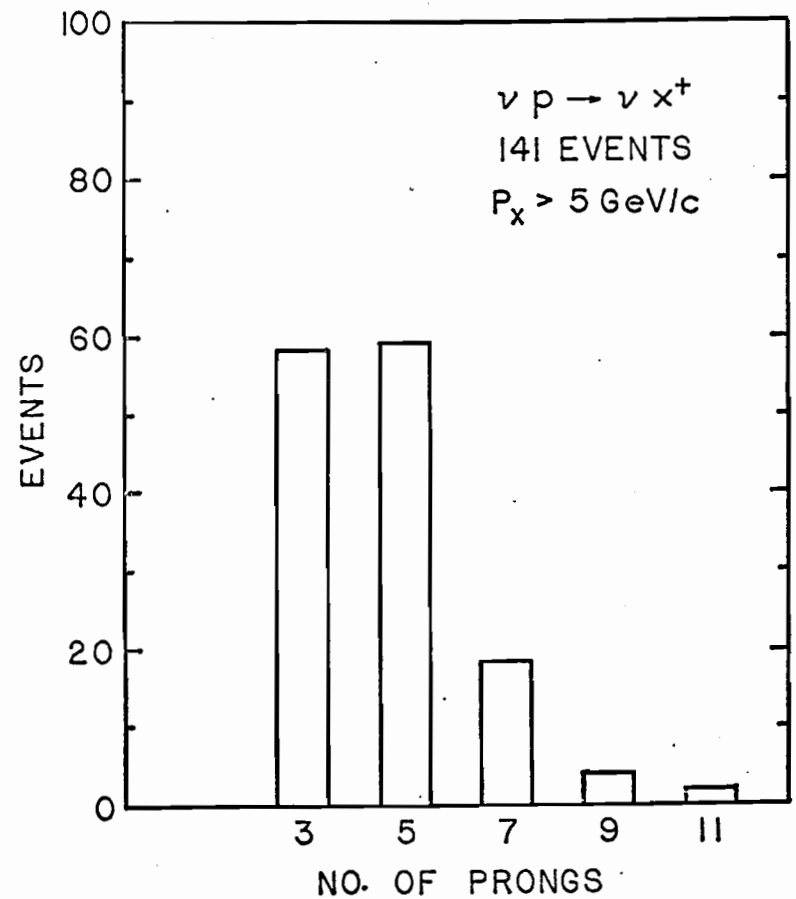
$\nu p \rightarrow \nu x^+$
141 EVENTS
$P_x > 5$ GeV/c
EVENTS
NO. OF PRONGS

fig. 4

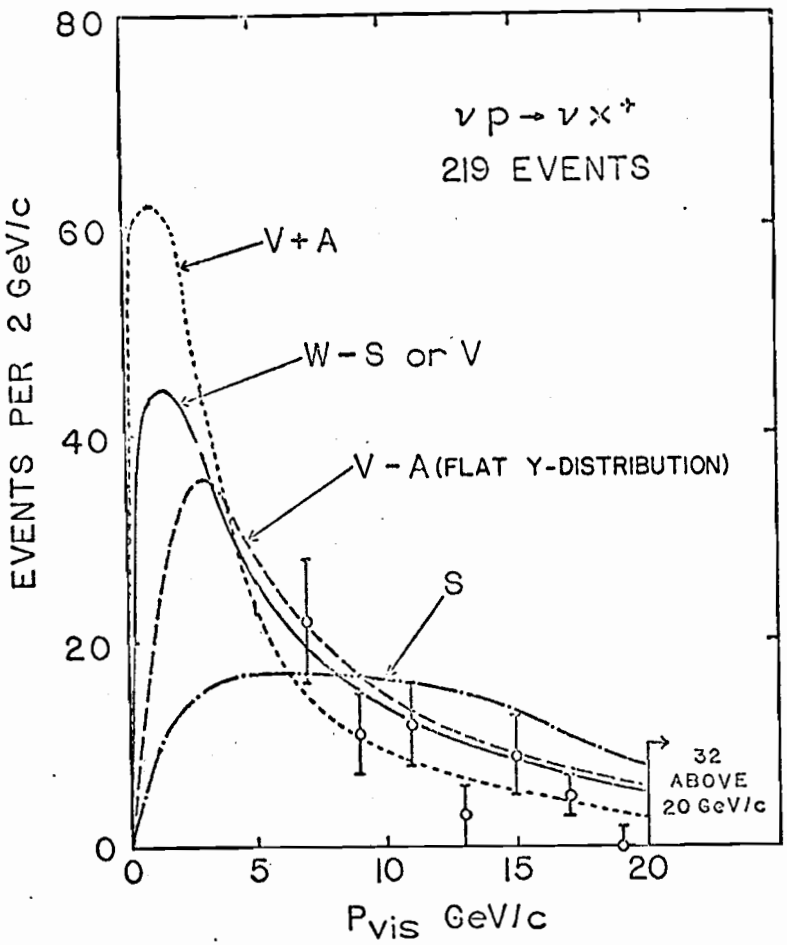
$\nu p \to \nu x^+$
219 EVENTS
V+A
W-S or V
V-A (FLAT Y-DISTRIBUTION)
S
32 ABOVE 20 GeV/c
EVENTS PER 2 GeV/c
P_{vis} GeV/c
0
20
40
60
80
0
5
10
15
20

fig. 5

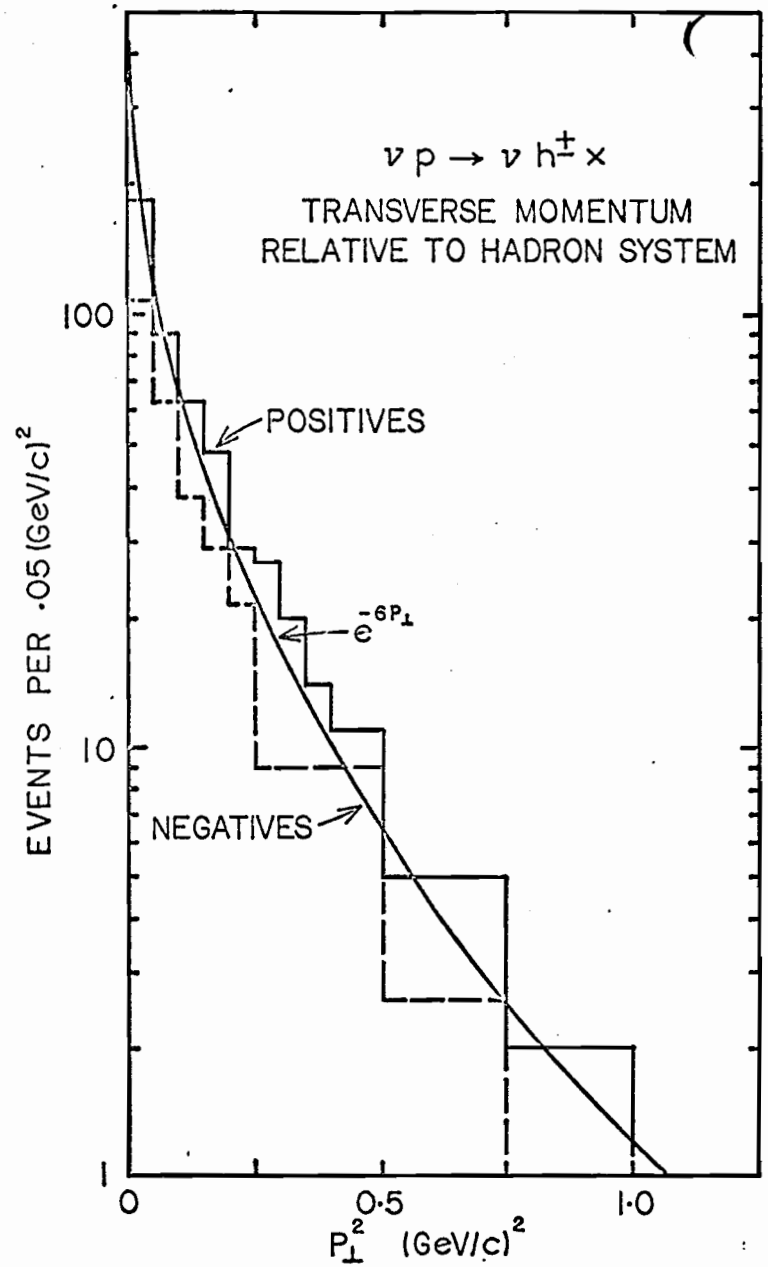
$\nu p \to \nu h^{\pm} x$
TRANSVERSE MOMENTUM
RELATIVE TO HADRON SYSTEM
POSITIVES
$e^{-6P_\perp}$
NEGATIVES
EVENTS PER .05 (GeV/c)^2
$P_\perp^2$ (GeV/c)^2
1
10
100
0
0·5
1·0

fig. 6

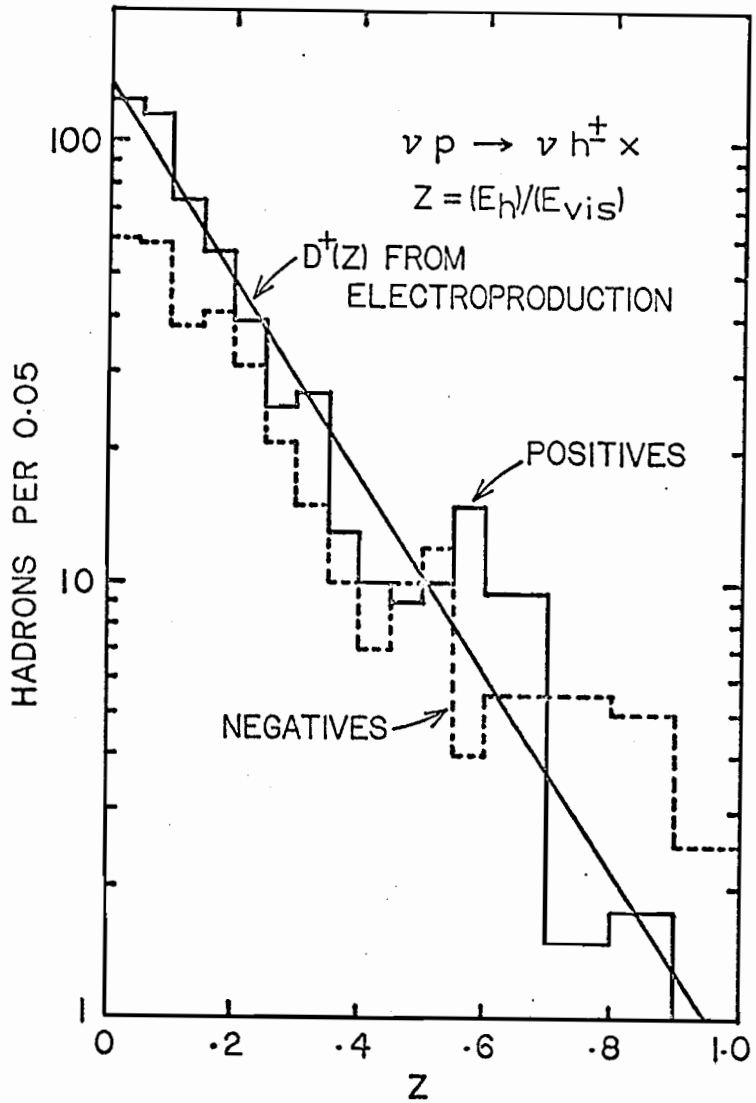
$\nu p \rightarrow \nu h^{\pm} x$
$Z = (E_h)/(E_{vis})$
$D^+(Z)$ FROM ELECTROPRODUCTION
POSITIVES
NEGATIVES
HADRONS PER 0·05
100
10
1
0
·2
·4
·6
·8
1·0
Z

fig. 7

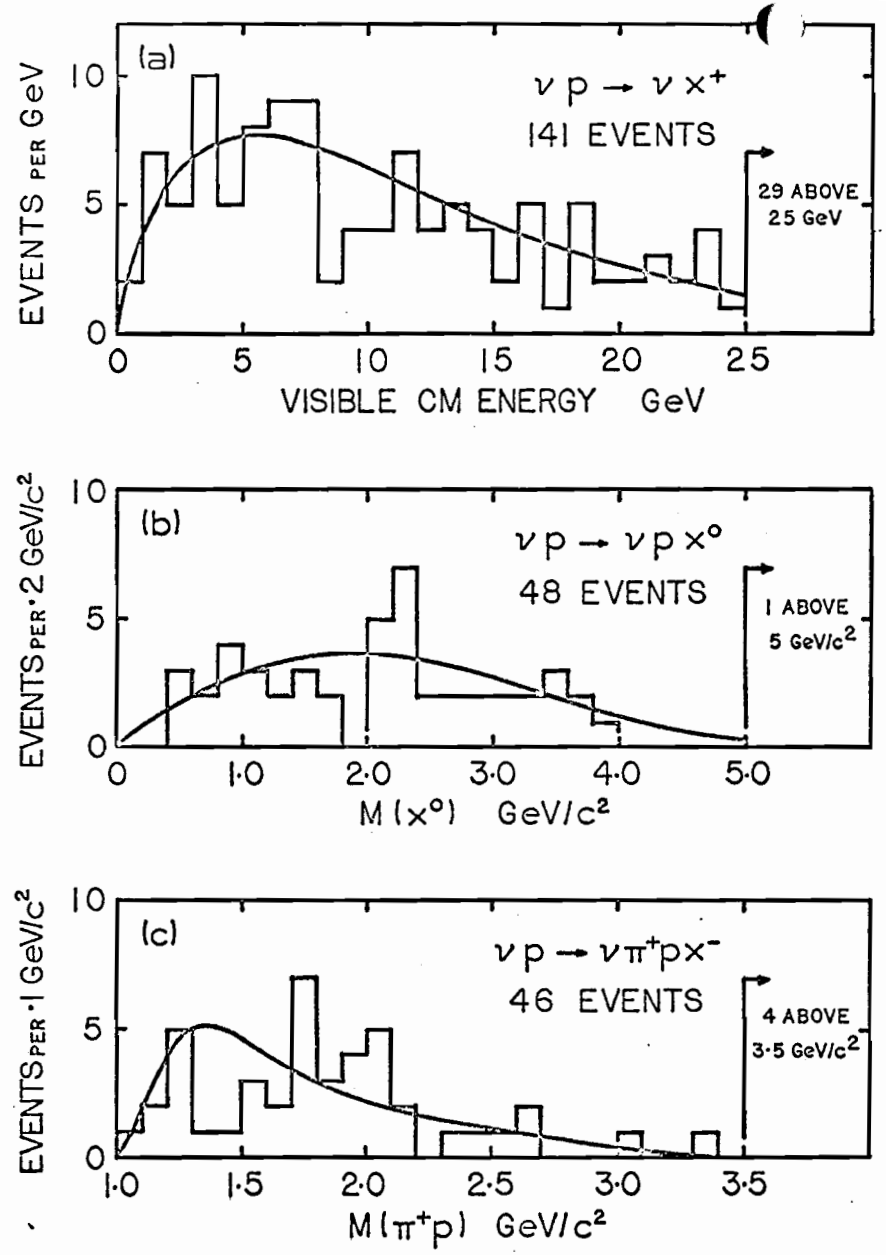
(a)
$\nu p \rightarrow \nu x^+$
141 EVENTS
29 ABOVE 25 GeV
EVENTS PER GeV
VISIBLE CM ENERGY GeV
(b)
$\nu p \rightarrow \nu p x^0$
48 EVENTS
1 ABOVE 5 GeV/c²
EVENTS PER 2 GeV/c²
M (x°) GeV/c²
(c)
$\nu p \rightarrow \nu \pi^+ p x^-$
46 EVENTS
4 ABOVE 3·5 GeV/c²
EVENTS PER 1 GeV/c²
M (π⁺p) GeV/c²

fig. 8

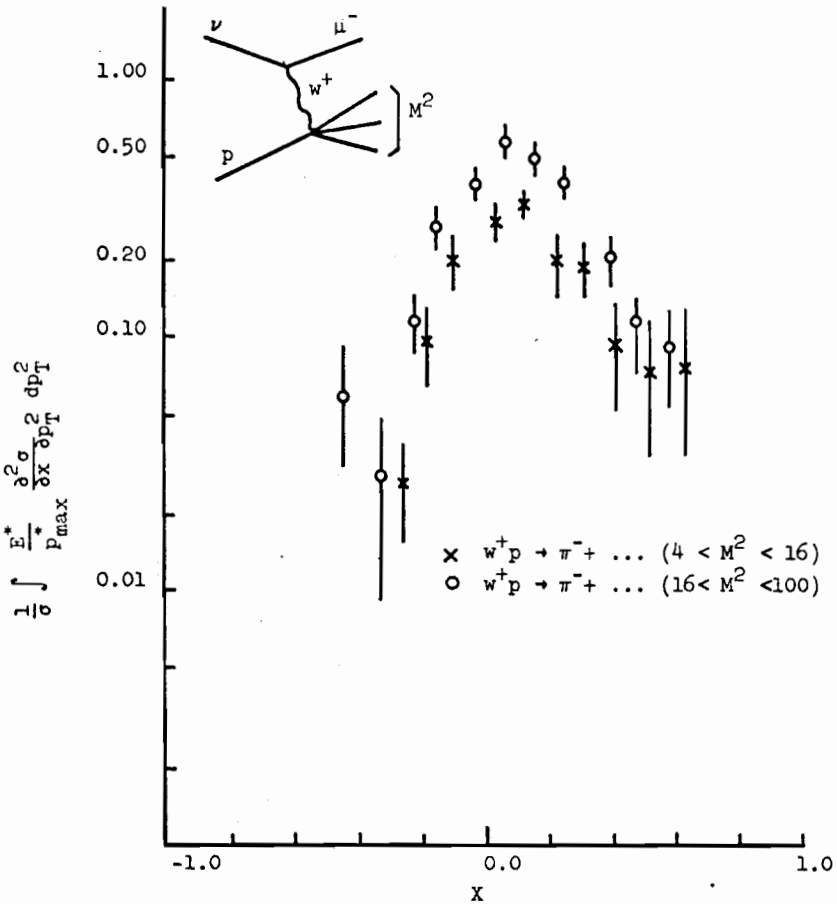
ν
μ⁻
w⁺
p
M²
1.00
0.50
0.20
0.10
0.01
× w⁺p → π⁻+ ... (4 < M² < 16)
o w⁺p → π⁻+ ... (16< M² <100)
-1.0
0.0
1.0
X

fig. 9

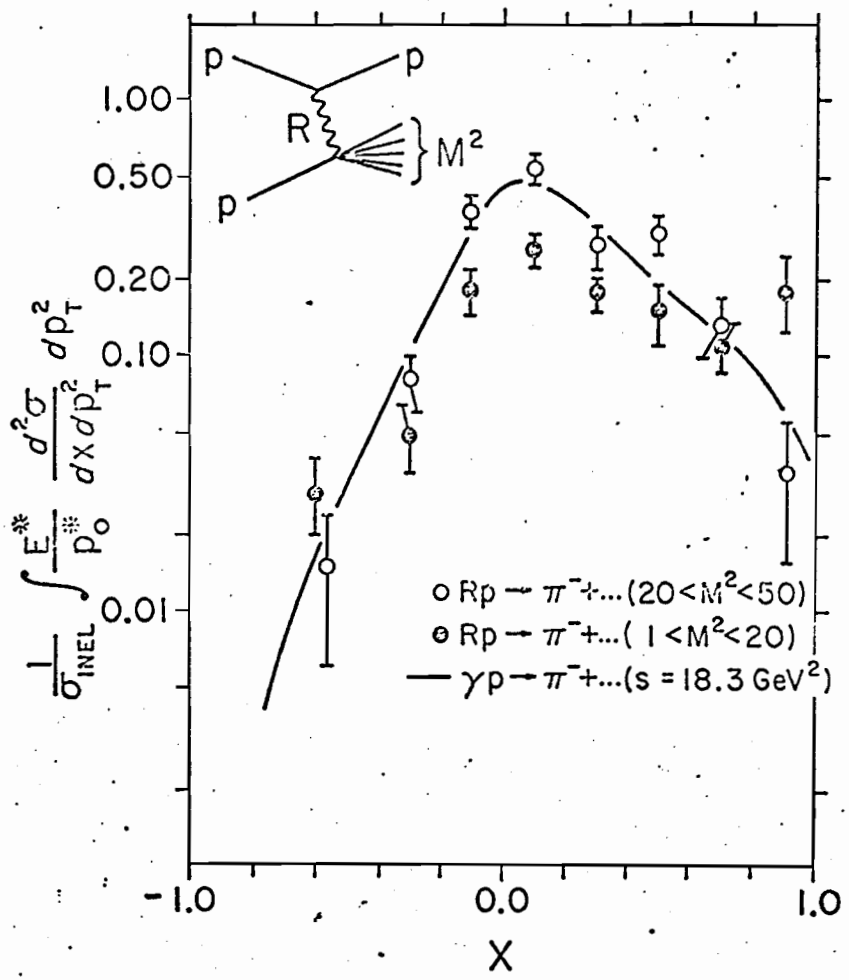
p
p
R
M²
p
1.00
0.50
0.20
0.10
0.01
o Rp → π⁻+...(20<M²<50)
⊖ Rp → π⁻+...(1 <M²<20)
— γp → π⁻+...(s = 18.3 GeV²)
-1.0
0.0
1.0
X

fig. 10

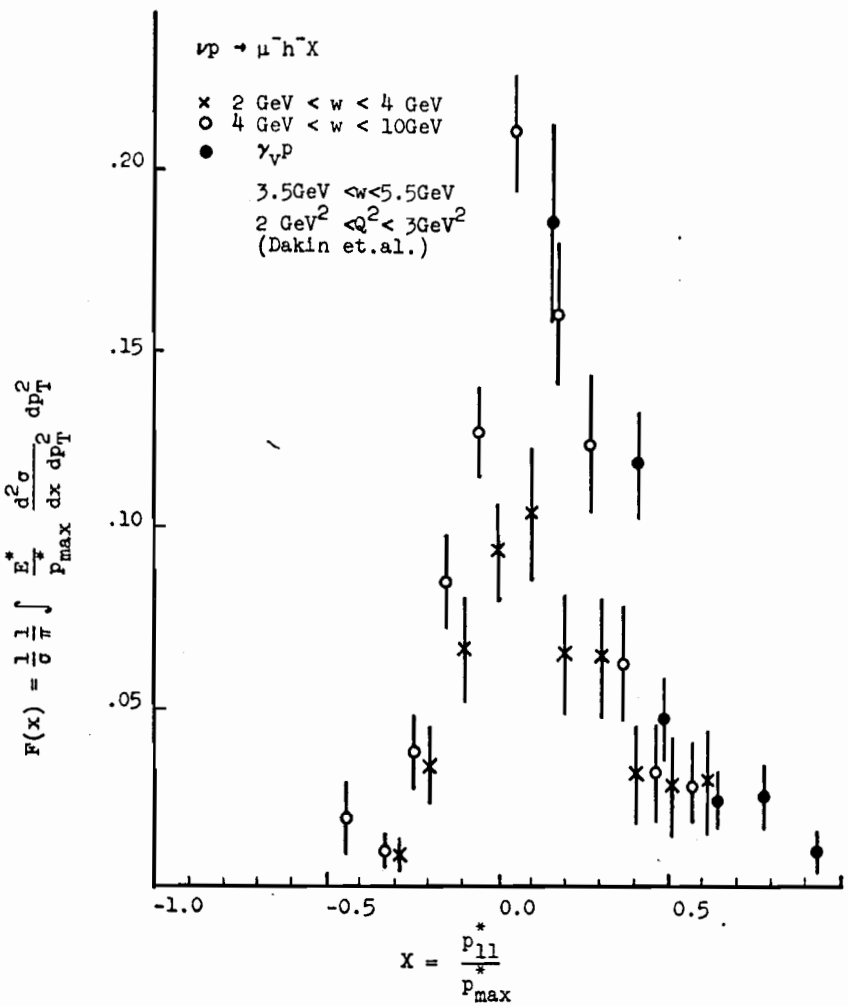
$\nu p \to \mu^- h^- X$
× 2 GeV < w < 4 GeV
○ 4 GeV < w < 10GeV
● $\gamma_V p$
3.5GeV <w<5.5GeV
2 GeV^2 <Q^2< 3GeV^2
(Dakin et.al.)
.20
.15
.10
.05
-1.0
-0.5
0.0
0.5
$F(x) = \frac{1}{\sigma}\frac{1}{\pi}\int \frac{E^*_\pi}{p_{max}} \frac{d^2\sigma}{dx\, dp_T^2} dp_T^2$
$X = \frac{p^*_{11}}{p^*_{max}}$

fig. 11

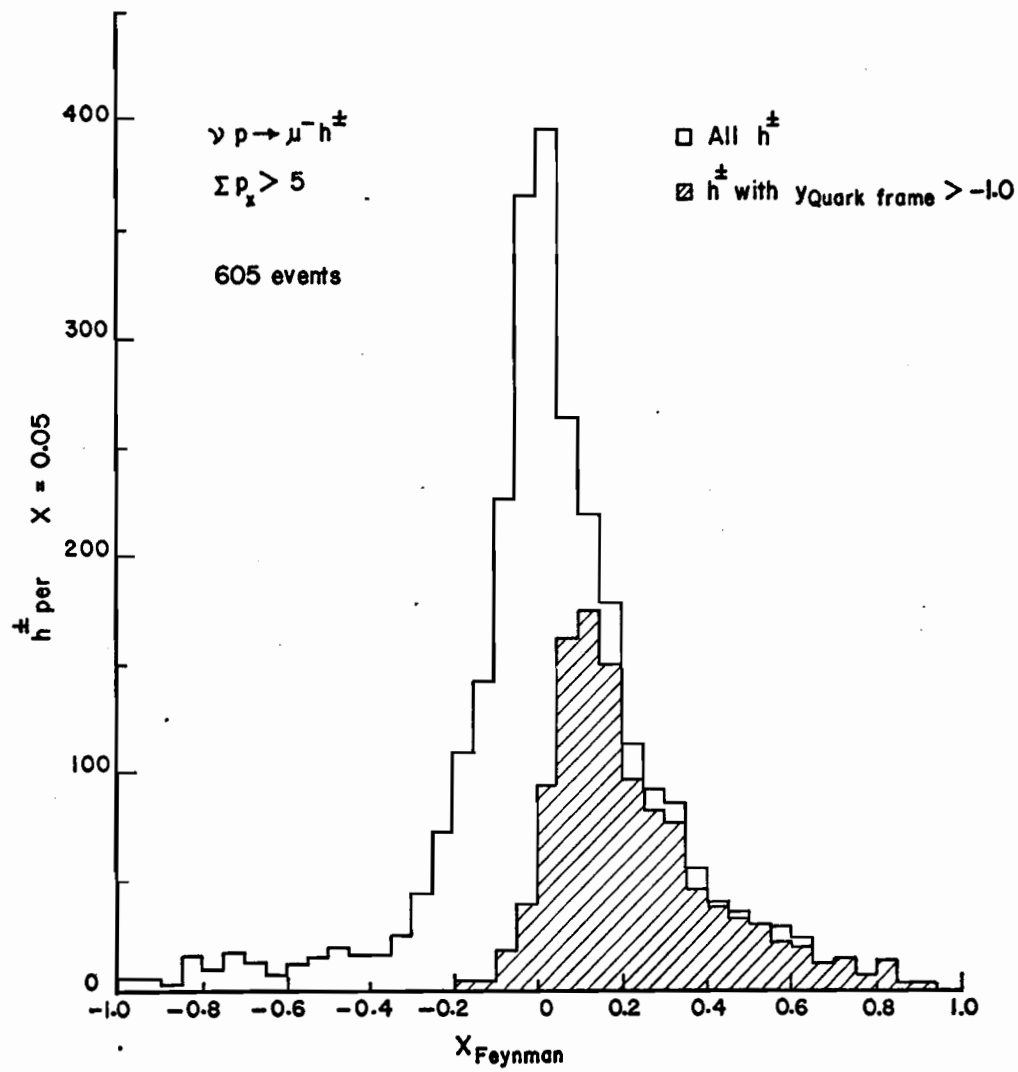
$\nu p \to \mu^- h^\pm$
$\Sigma p_x > 5$
605 events
□ All $h^\pm$
▨ $h^\pm$ with $y_{Quark\ frame} > -1.0$
400
300
200
100
0
$h^\pm$ per X = 0.05
-1.0
-0.8
-0.6
-0.4
-0.2
0
0.2
0.4
0.6
0.8
1.0
$X_{Feynman}$

fig. 12

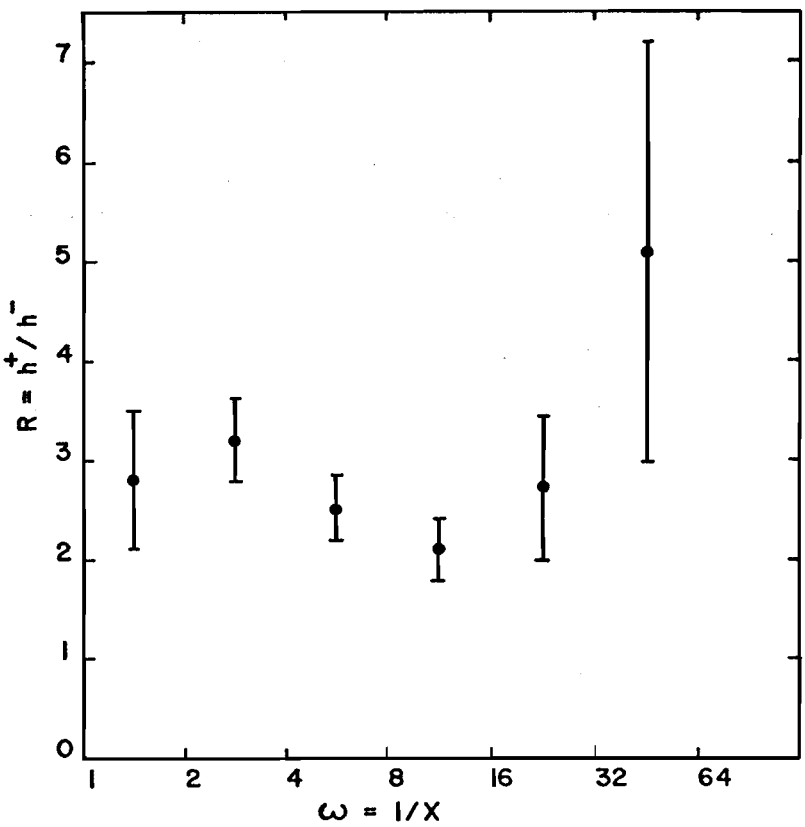
R = h+/h−
ω = 1/X
0
1
2
3
4
5
6
7
1
2
4
8
16
32
64

fig. 13

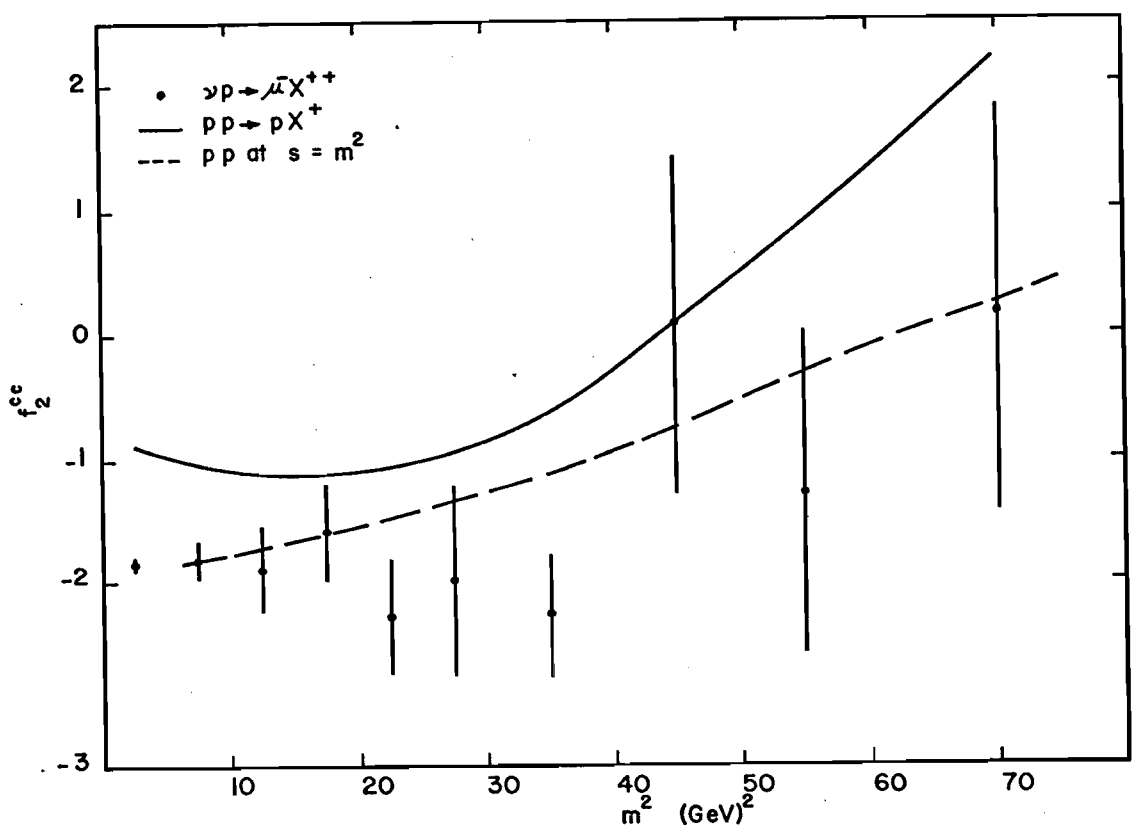
νp → μ⁻X⁺⁺
pp → pX⁺
pp at s = m²
f₂ᶜᶜ
m² (GeV)²
2
1
0
-1
-2
-3
10
20
30
40
50
60
70

fig. 14

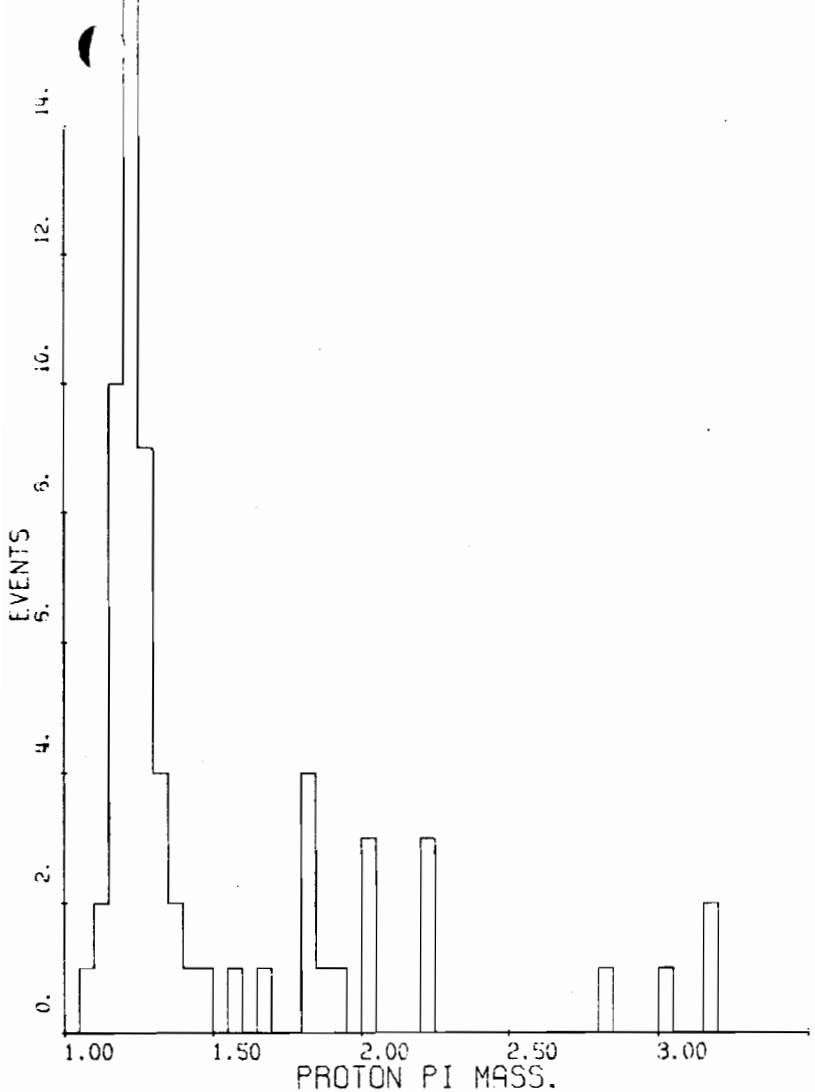
EVENTS
0.
2.
4.
6.
8.
10.
12.
14.
1.00
1.50
2.00
2.50
3.00
PROTON PI MASS.

fig. 15

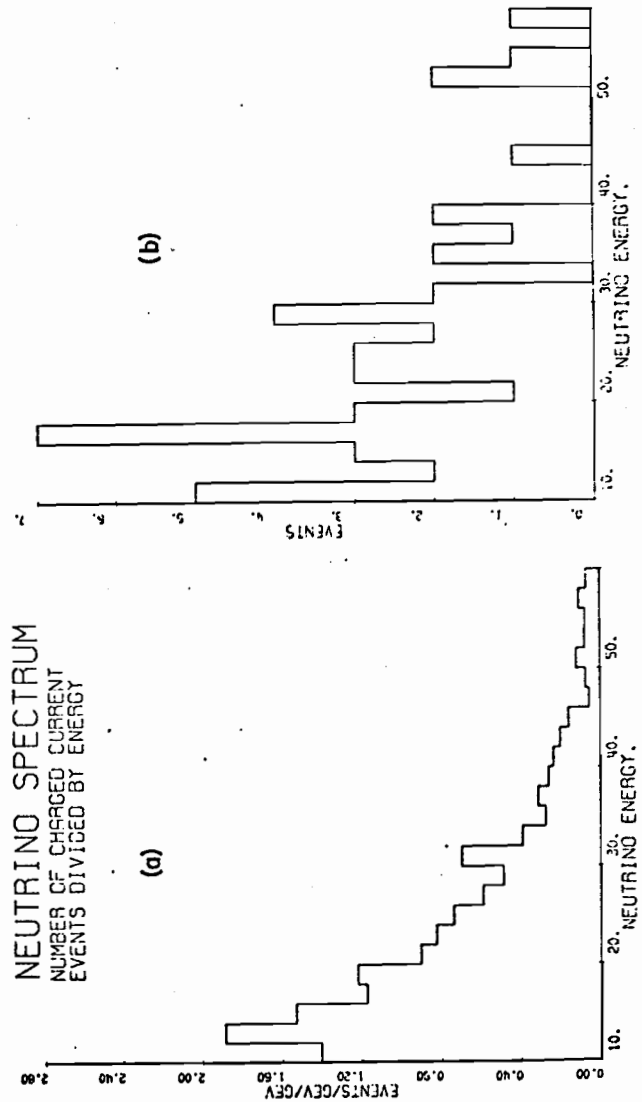
NEUTRINO SPECTRUM
NUMBER OF CHARGED CURRENT
EVENTS DIVIDED BY ENERGY
(a)
EVENTS/GEV/GEV
0.00
0.40
0.80
1.20
1.60
2.00
2.40
2.80
10.
20.
30.
40.
50.
NEUTRINO ENERGY.
(b)
EVENTS
0.
1.
2.
3.
4.
5.
6.
7.
10.
20.
30.
40.
50.
NEUTRINO ENERGY.

fig. 16

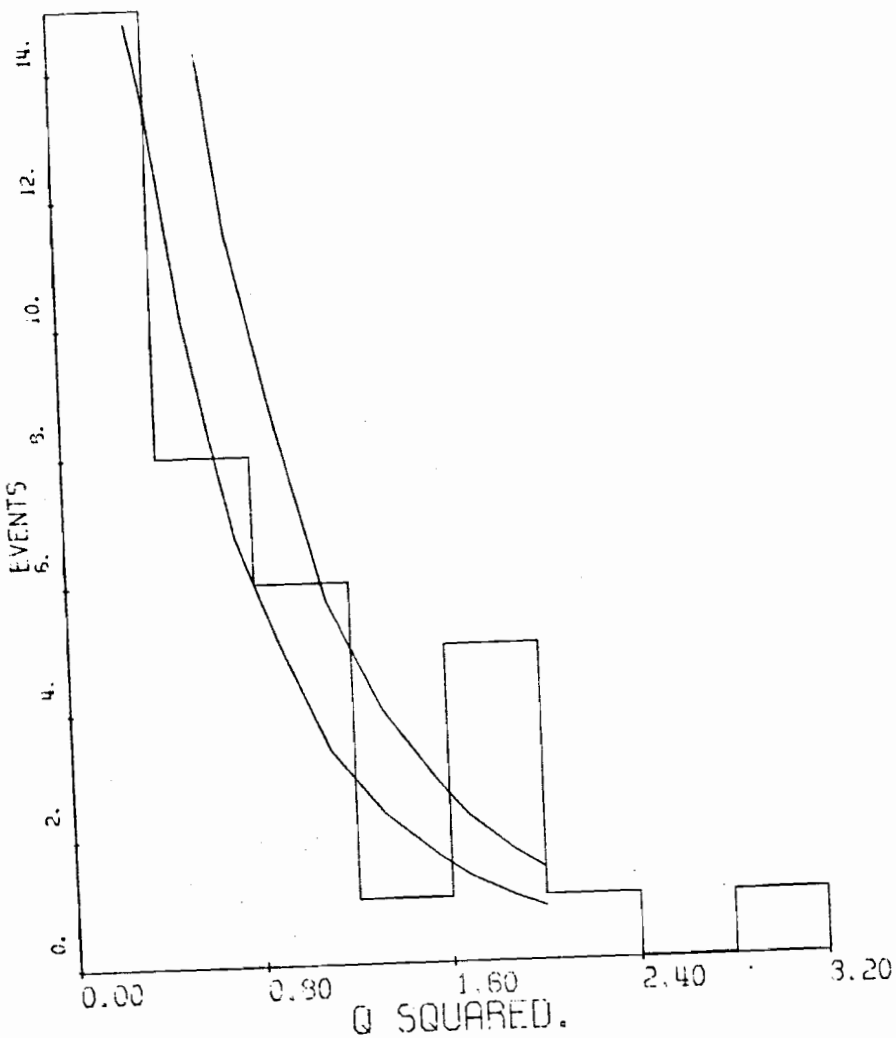
EVENTS
0.
2.
4.
6.
8.
10.
12.
14.
0.00
0.80
1.60
2.40
3.20
Q SQUARED.

fig. 17

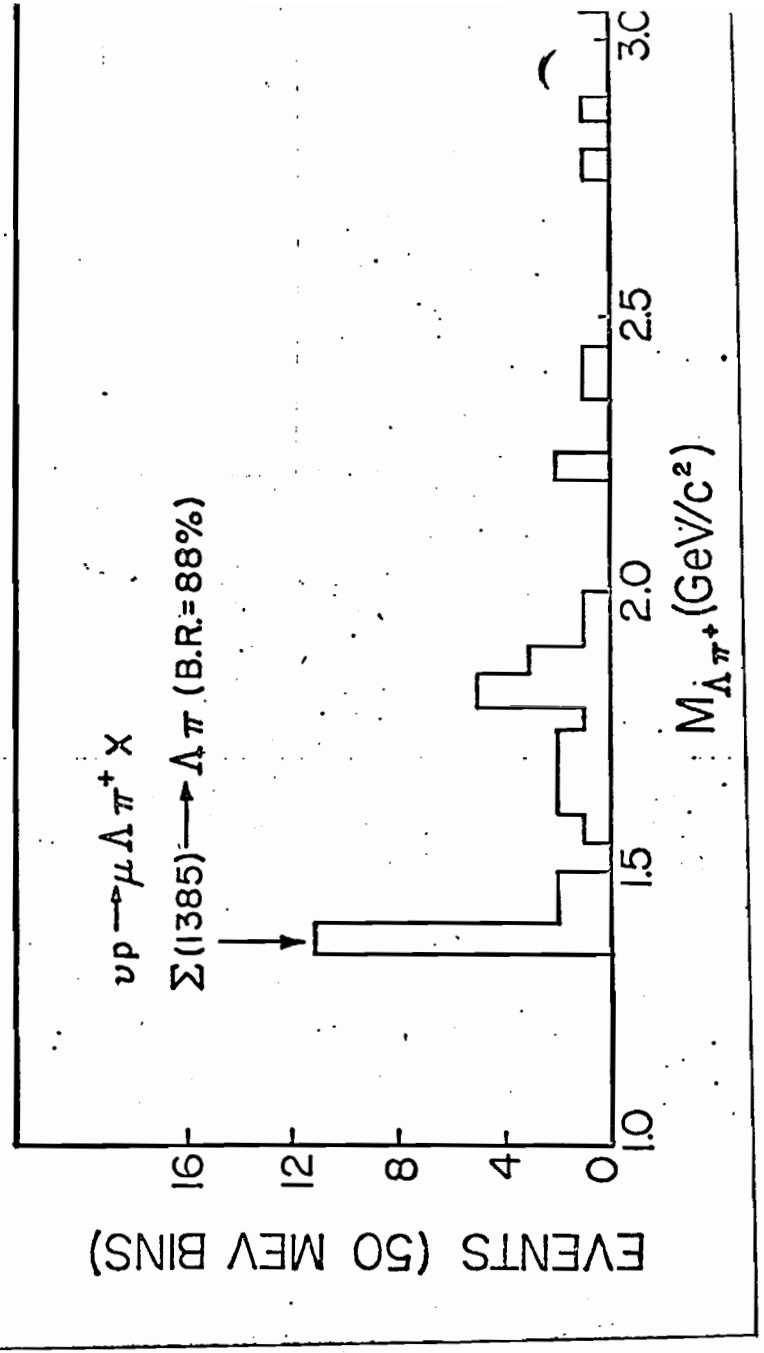
EVENTS (50 MEV BINS)
0
4
8
12
16
1.0
1.5
2.0
2.5
3.0
$M_{\Lambda\pi^+}$ (GeV/c²)
$\nu p \longrightarrow \mu \Lambda \pi^+ X$
$\Sigma(1385) \longrightarrow \Lambda\pi$ (B.R.=88%)

fig. 18